Magnetization and conductivity for $La_{1-x}Sr_xMnO_3$-type crystals

R. Allub and B. Alascio
Centro Atómico Bariloche, (8400) S. C. de Bariloche, Argentina
(Received 25 July 1996; revised manuscript received 7 February 1997)

We use a model previously formulated based on the double-exchange mechanism and diagonal disorder to calculate magnetization and conductivity for $La_{1-x}Sr_xMnO_3$-type crystals as a function of temperature. We use the results of the model to draw phase diagrams and we calculate the resistivity for different concentrations and magnetic fields and compare with experiment. [S0163-1829(97)07321-9]

The discovery of ''colossal'' magnetoresistance in $La_{1-x}Sr_xMnO_3$-type compounds[1] and its relation to possible applications of magnetoresistance (MR) devices has attracted the attention of the physics community in recent years. Before the discovery of ''colossal'' MR, the earlier studies by Jonker and van Santen[2] established a temperature-doping phase diagram separating the metallic ferromagnetic from the insulating antiferromagnetic phases. Zener[3] proposed a ''double-exchange'' (DE) mechanism to understand the phase diagram of these compounds and the intimate link between their magnetic and transport properties. This DE mechanism was used by Anderson and Hasegawa[4] to calculate the ferromagnetic interaction between two magnetic ions and by de Gennes[5] to propose canting states for weakly doped compounds. Kubo and Ohata[6] used a spin wave approach to study the temperature dependence of the resistivity at temperatures well below the critical temperature and a mean-field approximation at T near T_c. Mazzaferro *et al.*[7] used a mixed valence approach similar to that devised for TmSe combining DE with the effect of doping to propose the possibility of a metal-insulator transition in these compounds.

From the theoretical point of view, Furukawa[8] has shown that DE is essential to the theory of these phenomena, while Millis *et al.*[9] have argued that DE alone is not sufficient to describe the properties of some of the alloys under consideration and have proposed that polaronic effects play an important role. Müller-Hartmann and Dagotto[10] have pointed out that a new phase appears in the proper derivation of the effective hopping, but have not studied its effect in the physical properties of the systems under consideration.

In Ref. 11 we treated a model Hamiltonian proposed for these systems using an alloy analogy approximation to the exchange terms and including the effects of disorder by introducing a continuous distribution of the diagonal site energies. Here we continue that treatment by proposing a free energy that allows us to determine the magnetization as a function of temperature. We then proceed to find the Fermi energy and the mobility edge (ME) as functions of temperature. Finally, assuming that the conductivity is dominated by particles occupying extended states, we draw resistivity vs temperature curves. We compare our results with experiments in single crystals of $La_{1-x}Sr_xMnO_3$ reported by Tokura *et al.*[12] for four different values of the concentration of Sr and four different values of the magnetic field finding that the model allows a clear and coherent description of the experimental results showing the transition from metallic to insulating and the different shapes of the curves for different doping concentrations. This is possible within the calculation presented here for Sr-doped $LaMnO_3$ crystals, but it is not appropriate to describe samples where variable range hopping is found.

Our model Hamiltonian[11] is given by

$$H_m=\sum_{i,\mu}\epsilon_i n_{i\mu}-t\sum_{\langle i,j\rangle,\mu}c^{\dagger}_{i\mu}c_{j\mu}+\sum_i (Un_{i\uparrow}n_{i\downarrow}-J\vec{S_i}.\vec{\sigma_i}),$$

where we use the same notation and $n_{i\mu}=c^{\dagger}_{i\mu}c_{i\mu}$. We obtain site Green functions and thus local density of states for this problem. The electronic structure of the compounds consists of essentially four bands, two for spin up and two for spin down, the splitting between the up and down bands is given by the intra-atomic exchange energy J, their weight and width by the normalized magnetization $m=2\langle S\rangle$. The Fermi level always falls in the lower bands so that the transport properties are determined by these bands. Consequently, for $J\gg\sqrt{K}t$, where K is the connectivity, using the site density of state [Eq. (11) in Ref. 11] the averaged density of states per site reduces to

$$\rho_{0\mu}(\omega)=\frac{\nu_\mu(K+1)\sqrt{4Kt^2\nu_\mu-(\omega-E)^2}}{2\pi|(K+1)^2t^2\nu_\mu-(\omega-E)^2|}, \qquad (1)$$

where $E=(\epsilon-J)$ and $\nu_\mu=(1+\mu\ m)/2$ ($\mu=\pm$ for up and down spin respectively).

We introduce the effect of the disorder originated by the substitution of some of the rare-earth ions by Sr, Ba, or Ca. We assume that this can be described within the model by making the diagonal energies site dependent. As is well known since Anderson's original paper[13] a distribution of diagonal energies produces localization of the electronic states from the edges of the bands to an energy within them which is called the ''mobility edge'' (ME). The precise position of the ME is difficult to calculate and different localization criteria result in different values for it.[14] However, we do not aim here for an absolute value for the ME but rather to its change with respect to the Fermi level when the magnetization changes from saturation to zero. For this reason we assume that there is no localization before disorder and for simplicity, we use a Lorentzian distribution of energies[15] and the Ziman criterium of localization.[16] From the ensemble-averaged Green function we obtain densities of

states $\rho_\mu(\epsilon)=\int_{-\infty}^{+\infty}\rho_{0\mu}(\epsilon')L(\epsilon-\epsilon')d\epsilon'$, where $L(x)$ is a Lorentz distribution of width Γ.

Within this *comparative* approach one can make the further approximation replacing $\rho_{0\mu}$ by a square density of states with the same width $W_\mu=2t\sqrt{K\nu_\mu}$ and the same weight ν_μ to obtain

$$\rho_\mu(\epsilon)=\frac{\nu_\mu}{2\pi W_\mu}\{\arctan[(W_\mu-\epsilon)/\Gamma]+\arctan[(W_\mu+\epsilon)/\Gamma]\},$$

which allows for analytical expressions for the number of particles n, and the internal energy E as functions of the magnetization m, and the Fermi energy ϵ_F. In some instances, when the Fermi level falls too near the band edge, this approximation can differ from the more realistic case where the density of states increases as $\sqrt{\epsilon}$. We will see below that this is the case for $n=0.15$ in the samples we use to compare our results with.

To proceed further, we need an expression for the entropy of these systems. Again for *comparative* purposes, we resort to the simplest possible form compatible with our earlier approximations, that of a spin-1/2 array of sites: $S=\ln(2)-\nu_+\ln(2\nu_+)-\nu_-\ln(2\nu_-)$. More accurate forms of the entropy valid in the mixed valence regime can be used, see, for example, Ref. 17. In the presence of a magnetic field H, the free energy per site is $G=E-TS-\mu_B mH$, where T is the temperature and μ_B is the magnetic moment per site.

We proceed as follows. For each n, we use (assuming $k_BT\ll W_\sigma$) $n=\Sigma_\mu\int_{-\infty}^{\epsilon_F}\rho_\mu(\epsilon)d\epsilon$ to obtain a relation between n,m, and ϵ_F from which ϵ_F can be determined numerically. The free energy is then a function of m and T only and allows, by minimization, us to determine $m(T)$. The resulting $m(T)$ (Shown in Fig. 1) does not differ essentially from the law of corresponding states for spin 1/2. Having obtained $m(T)$ for each value of the parameters we can determine the up and down mobility edges (B_+ and B_-) and the Fermi energy. They are also plotted as functions of temperature in Fig. 1.

Following Mott and Davies[18] we calculate the transport properties assuming that two forms of dc conduction are possible: thermally activated hopping and excitation to the mobility edge. When the difference between the Fermi level and the mobility edge Δ is not too large as compared tok_BT , the conductivity is dominated by particles in the extended states, and is given by the usual relaxation time form $\sigma=(e^2/3a^3)\Sigma_\mu\{\int_{-\infty}^{\infty}v_\mu^2(\epsilon)\tau_\mu(\epsilon)\rho_\mu(\epsilon)[-(\partial f(\epsilon)/\partial\epsilon)]d\epsilon\}$, in which a is the Mn-Mn distance in the simple cubic lattice, $f(\epsilon)$ is the Fermi function. We assume that the relaxation time τ_μ is a step function equal to zero for $\epsilon<B_\mu$ and takes a value τ_0 related to the minimum metallic conductivity for $\epsilon>B_\mu$, where, according to Ref. 15, $B_\mu=-\sqrt{t^2K^2\nu_\mu-\Gamma^2}$. We further replace $v_\mu(\epsilon)$ by its average $v_\mu^2=W_\mu^2a^2/2\hbar^2$ to obtain

$$\sigma=\frac{e^2\tau_o}{6\hbar^2a}*\sum_\mu\left\{W_\mu^2*\int_{B_\mu}^{\infty}\rho_\mu(\epsilon)\left(-\frac{\partial f(\epsilon)}{\partial\epsilon}\right)d\epsilon\right\}. \quad (2)$$

An Anderson transition takes place when B_μ vanishes. For $(t^2K^2\ \nu_\mu-\Gamma^2)<0$ all eigenstates became localized.

In what follows we take $K=5$ appropriate to describe the simple cubic lattice of the Mn sites and $t=1$ fixes the scale of energies. As a consequence of the structure of the model and of the approximations that led us to this point, the model becomes symmetric under electron-hole transformation in the lower spin up and down bands.

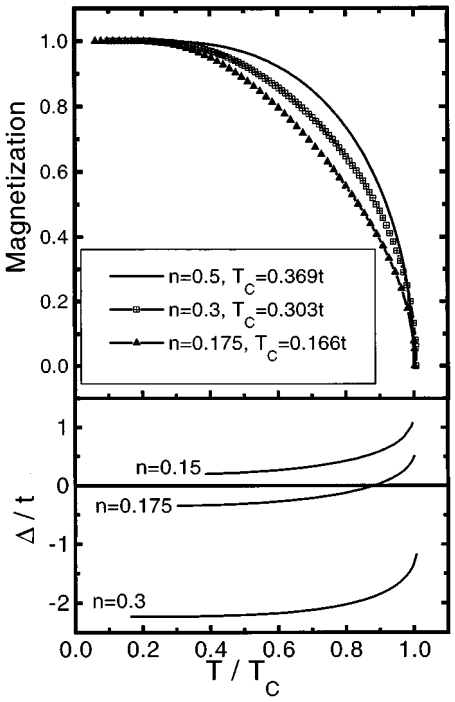

FIG. 1. Zero-field magnetization (upper panel) and $\Delta=(B_+-\epsilon_F)$ (lower panel) are plotted as a function of the normalized temperature (T/T_C) for $\Gamma=1.8$, $K=5$, $t=1$, and different values of doping n.

For $n=0.5$, the Fermi energy vanishes independently of the value of the magnetization and one can obtain an analytical expression for the free energy, from which we derive T_C:

$$T_C=[(\Gamma^2+30t^2)\arctan(\sqrt{10}t/\Gamma)-\Gamma\sqrt{10}t]/(8\pi\sqrt{10}t).$$

Connected to the transport properties we can define a characteristic temperature T_M at which the mobility edge crosses the Fermi level. Notice, however, that this crossing does not imply any discontinuous change in the resistivity, the only nonanalyticity occurs at T_C. For $n=0.5$ we obtain an explicit expression for T_M:

$$T_M=\frac{\Sigma_\mu\mu[(3A_\mu^2-\Gamma^2)\arctan(A_\mu/\Gamma)-2A_\mu\Gamma\ln(A_\mu^2+\Gamma^2)]}{4\pi\ln[(1+m_c)/(1-m_c)]},$$

where $A_\mu=2t\sqrt{Km_\mu}$, $m_\mu=(1+\mu\ \ m_c)/2$, and $m_c=(2\Gamma^2/t^2K^2)-1$. In Fig. 2 we show T_C and T_M as a function of Γ for $n=0.5$.

In what follows we consider $n<0.5$ and identify n with the number of holes, which we take to be equal to the concentration of the divalent component of the alloy. We define as insulator the state where the Fermi level falls below the ME $[\Delta=(B_+-\epsilon_F)>0]$, so that, for small Γ, the Fermi level falls above the ME ($\Delta<0$) and only the metallic state appears. When Γ increases, Δ reduces and finally $\Delta=0$ for a critical value $\Gamma_-=\sqrt{0.5K^2t^2-\epsilon_F^2}$ (where $m_c=0$ and

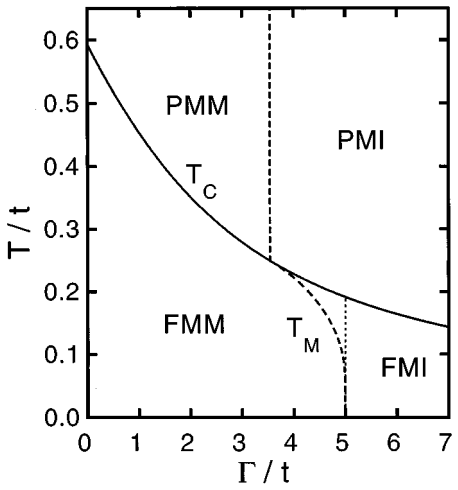

FIG. 2. Phase diagram for $n=0.5$ ($\epsilon_F=0$). Ferromagnetic T_C (solid line) and metal-to-insulator T_M (dashed line) transition temperatures vs Γ for $H=0$, $K=5$, and $t=1$. Regions are labeled FMM (ferromagnetic metal: $m\neq 0$ and $\Delta<0$), FMI (ferromagnetic insulator: $m\neq 0$ and $\Delta>0$), PMM (paramagnetic metal: $m=0$ and $\Delta<0$), and PMI (paramagnetic insulator: $m=0$ and $\Delta>0$). The dotted line is a guide to the eye.

$T_C=T_M$). When Γ is increased from Γ_-, T_M reduces and finally $T_M=0$ at a critical value $\Gamma_+=\sqrt{K^2t^2-\epsilon_F^2}$. Above Γ_+ the system remains insulating at all temperatures. Consequently, only for $\Gamma_-<\Gamma<\Gamma_+$ does the transition between metallic and insulating regimes appear. All these facts are depicted in Fig. 2 for $n=0.5$ ($\epsilon_F=0$). Note the similarity of T_c vs Γ with T_c versus electron-phonon coupling in Ref. 9.

In Fig. 3 we show T_C and T_M as functions of n for some values of Γ. As a consequence of the density of states being

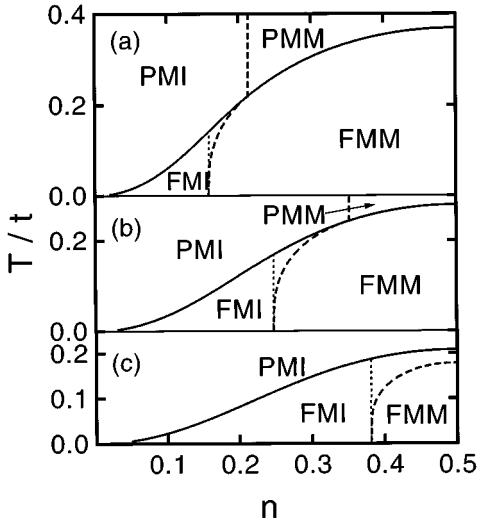

FIG. 3. Phase diagram. Ferromagnetic T_C (solid lines) and metal-to-insulator T_M (dashed lines) transition temperatures vs doping n for $H=0$, $K=5$, $t=1$, and different values of Γ: (a) $\Gamma=1.8$, (b) $\Gamma=3$, and (c) $\Gamma=4.5$. Regions are labeled as FMM (ferromagnetic metal: $m\neq 0$ and $\Delta<0$), FMI (ferromagnetic insulator: $m\neq 0$ and $\Delta>0$), PMM (paramagnetic metal: $m=0$ and $\Delta<0$), and PMI (paramagnetic insulator: $m=0$ and $\Delta>0$). The dotted lines are a guide to the eye.

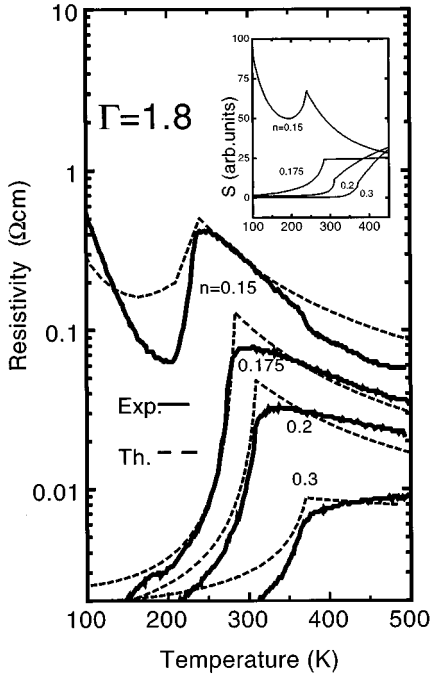

FIG. 4. Zero-field resistivity (solid lines) on a logarithmic scale vs temperature in La_{1-n} Sr_nMnO_3taken from Ref. 12. The dashed lines represent the fits with Eq. (10) for $t=1$, $\Gamma=1.8$, $K=5$, and the corresponding values of doping: $n=0.15$, $n=0.175$, $n=0.2$, and $n=0.3$. Inset: Thermopower for the same values of n in arbitrary units as a function of temperature.

modified by disorder, the Curie temperatures decrease with Γ, while the increase with n is just a consequence of the energetics of the bands. Tentative fitting of the calculated resistivity with the data on $La_{1-x}Sr_xO_3$ of Ref. 12 gives a value of $1.8t$ for Γ.

In Fig. 4 we have tried tentatively to fit the logarithm of the resistivity as obtained from Eq. (2) to the measurements of Tokura *et al.*[12] We have chosen to compare with these samples to avoid the complications that arise from strong coupling to the lattice in the smaller radius compounds.[19] To do that, we fix arbitrarily the value of Γ at $1.8t$. We let t vary from sample to sample to fit T_c. Starting with the curve corresponding to x or $n=0.175$ we choose $t=1704$ K and change to $t=1529$ K for $n=0.2$, to $t=1216$ K for $n=0.3$, and to $t=1600$ K for $n=0.15$. These values of t correspond to bandwidths that range between 1.3 to 0.93 eV. We then multiply the values of each calculated resistivity by a constant (in the logarithmic plot this corresponds to shifting the curves up and down) to fit approximately the value at the maximum. This last constant corresponds to different values of τ_0 in Eq. (2) which range from 10^{-15} to 10^{-16} sec. These τ_0's correspond to the minimum conductivity defined in Mott and Davis.[18] We can see that the fitting is better in the more ''metallic'' samples than in the $n=0.15$ sample where one could expect the contribution of localized states to be larger and the model results differ more from experiment. Indeed, as pointed out above, the resistivity calculated with the square density of states differs even more from experiment than the one shown in Fig. 4, which is calculated with the more realistic density of states of Eq. (1).

We conclude from the comparison that the model allows

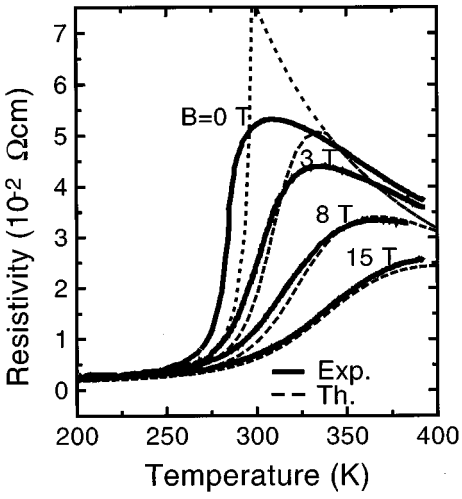

FIG. 5. Magnetoresistance in $La_{1-n}Sr_nMnO_3$ ($n=0.175$). The solid lines show the temperature dependence of resistivity in magnetic fields taken from Ref. 12. The dashed lines represent the fits with Eq. (10) for $t=1$, $\Gamma=1.75$, $K=5$, and the corresponding values of magnetic field: $B=0$, $B=3$ T, $B=8$ T, and $B=15$ T.

us to characterize the resistivity behavior of different samples by two parameters, one associated to the degree of disorder (Γ), and the other to the hopping energy t. The values of the hopping energy t can be affected by displacement of the oxygen atoms, or by polaronic or other many-body effects.

In Fig. 5 we show the magnetic-field effect on the resistivity and compare again with the results obtained in Ref. 12. Here again, we take $\Gamma=1.8$, $t=1789$ K, and select $\tau_0=0.96\times10^{-14}$ to fit the $H=8$ T curve. We take $\mu_B=0.964\times10^{-20}$ erg/G to fit the rest of the curves. Indeed, the fitting of resistivity curves in the absence of magnetic field should be taken with care because of the effect of magnetic domains walls.

Three main interactions should be incorporated in a more complete description of the whole family of ''colossal magnetoresistance '' Mn perovskites.

(1) Static and dynamic lattice effects can modify not only the values of both parameters t and Γ, but also the thermodynamics of the transition, leading to first-order transitions as those found in many of the compounds.[20] The connection to the dynamics of the lattice has been recently very elegantly demonstrated by Zhao *et al.*[21]

(2) Coulomb interactions between ions, that in combination with point (1) above could also produce charge ordering and lead to the reentrant behavior found in Ref. 20.

(3) Superexchange interactions between the localized spins that lead to canted states, as those found in electron-doped $Ca_{1-x}Y_xMnO_3$.[22]

The thermopower (S) can also be calculated following the same procedure and approximations. The results for this quantity are shown as an inset in Fig. 4. The correlation between ln (ρ) and S pointed out in Ref. 23 is apparent. Measurements of this quantity and resistivity in the same crystalline samples would be highly desirable.

To summarize, we have shown that a very simple estimation of the effect of disorder on the double-exchange mechanism allows us to understand resistivity and magnetoresistivity of Sr-doped La manganites. The most natural source of disorder is the substitution of rare earths by Sr, Ca, or Ba, but polaronic or other many-body effects may act in a similar way.

One of us (R.A.) was supported by the Consejo Nacional de Investigaciones Centífilos y Técnicas (CONICET), Argentina. B.A. was partially supported by CONICET.

[1] R. von Helmolt *et al.*, Phys. Rev. Lett. **71**, 2331 (1993).
[2] G. H. Jonker and J. H. van Santen, Physica **16**, 337 (1950); J. H. van Santen and G. H. Jonker, *ibid.* **16**, 599 (1950).
[3] C. Zener, Phys. Rev. **82**, 403 (1951).
[4] P. W. Anderson and H. Hasegawa, Phys. Rev. **100**, 675 (1955).
[5] P. G. de Gennes, Phys. Rev. **118**, 141 (1960).
[6] K. Kubo and N. Ohata, J. Phys. Soc. Jpn. **33**, 21 (1972).
[7] J. Mazzaferro *et al.*, J. Phys. Chem. Solids **46**, 1339 (1985).
[8] N. Furukawa, J. Phys. Soc. Jpn. **63**, 3214 (1994).
[9] A. J. Millis *et al.*, Phys. Rev. Lett. **74**, 5144 (1995).
[10] E. Müller-Hartmann and E. Dagotto, Phys. Rev. B **54**, R6819 (1996).
[11] R. Allub and B. Alascio, Solid State Commun. **99**, 613 (1996).
[12] Y. Tokura *et al.*, J. Phys. Soc. Jpn. **63**, 3931 (1994).
[13] P. W. Anderson, Phys. Rev. **109**, 1492 (1958).
[14] D. C. Licciardello and E. N. Economou, Phys. Rev. **11**, 3697 (1975).
[15] P. Lloyd, J. Phys. C **2**, 1717 (1969).
[16] J. M. Ziman, J. Phys. C **2**, 1230 (1969).
[17] A. A. Aligia, Ph.D. Thesis, Instituto Balseiro, 1984.
[18] N. F. Mott and E. A. Davis, *Electronic Processes in Non-Crystallyne Materials* (Oxford University Press, Oxford 1971).
[19] H. Y. Hwang *et al.*, Phys. Rev. Lett. **75**, 914 (1995).
[20] H. Kuwahara *et al.*, Science **270**, 961 (1995).
[21] Guo-meng Zhao *et al.*, Nature (London) **381**, 676 (1996).
[22] J. Briatico *et al.*, Czech. J. Phys. **46**, Suppl. S4, 2013 (1996).
[23] Baoxing Chen *et al.*, Phys. Rev. B **53,** 5094 (1996).